

# Neutrino/Electron Scattering Comparison

S. A. Wood<sup>a</sup>

<sup>a</sup>Thomas Jefferson National Accelerator Facility, 12000 Jefferson Avenue,  
Newport News, VA 23602, USA

The physics and practical aspects of electron and neutrino scattering experiments on nucleons and nuclei are compared. Methods of using electron scattering data to improve the nuclear physics in neutrino event generators are proposed.

## 1. Introduction

Because of the weak interaction probability of neutrinos, scattering neutrinos uniformly “illuminate” the nucleon or nucleus that they scatter from, thus directly probing parton or nucleon distributions. This is in contrast to hadrons which preferentially scatter from the front hemisphere of a nucleus due to their strong interaction probability. Electron scattering, while having complications due to electromagnetic divergences (discussed below), will couple in different ways, but still uniformly illuminate the target nucleus. This means that electron and neutrino scattering should exhibit the same nuclear effects, particularly final state interactions between the fragments of a struck nucleon or nucleus.

Monte-Carlo simulations of neutrino scattering, such as the NUANCE[1] or NEUGEN[2] event generators, play an important role in the analysis of neutrino experiments. These simulations use a variety of models of the nucleon and nucleus and of the interactions of hadrons knocked out of nuclei. The physics in these event generators is checked by comparing to various types of data such as hadron-nucleus scattering or neutrino scattering data itself. However, similarities of electron and neutrino interactions provide a unique opportunity to use the growing amount of precise electron scattering data to confirm or improve the physics in neutrino event generators.

## 2. Comparison of Electron and Neutrino Scattering

Electrons and neutrinos are leptons that both interact with matter via the electroweak force, i.e. coupling to the vector bosons,  $\gamma$ ,  $W^+$ ,  $W^-$ . Neutrinos can scatter via exchange of the massive  $Z_0$  (neutral current), or can charge exchange into a charged lepton via exchange of a  $W^+$  or  $W^-$ . Electrons (and other charged leptons) scatter primarily through exchange of massless photons although a small component of the amplitude proceeds through  $Z_0$  exchange. This component leads to a small parity violation effect that can be exploited for standard model tests[3], strange form factor measurements[4] or searches for new physics[5]. A powerful method of extracting nucleon information, such as parton distribution functions, is to combine results from experiments encompassing all four exchange bosons (charged lepton scattering, neutrino and anti-neutrino charge current scattering, and neutral current scattering).

One major source of differences in the scattering of these two types of leptons is in the propagators,  $1/Q^2$  for electron scattering and  $1/(Q^2 - M_{Z,W}^2)$  neutrino scattering. This has several implications, one being that, for  $Q^2 \ll M_{Z,W}^2$ , scattering cross sections are much larger for electrons than neutrinos. Furthermore, while the total cross section for neutrino scattering is finite at any given neutrino energy, electron scattering cross sections diverge at small scattering angles, so total cross sections are formally infinite.

When analyzing electron scattering data, the Mott cross section,

$$\sigma_M = \frac{4\alpha^2 E'^2 \cos^2 \theta/2}{Q^4} = \frac{\alpha^2 \cos^2 \theta/2}{4E^2 \sin^4 \theta/2}, \quad (1)$$

must be factored out first before extracting any “physics” such as form factors. The strong dependence of cross sections (and  $Q^2$ ) on electron scattering angle mean that the systematics of angle measurements must be carefully controlled, particularly when making measurements such to separate longitudinal and transverse form factors or structure functions.

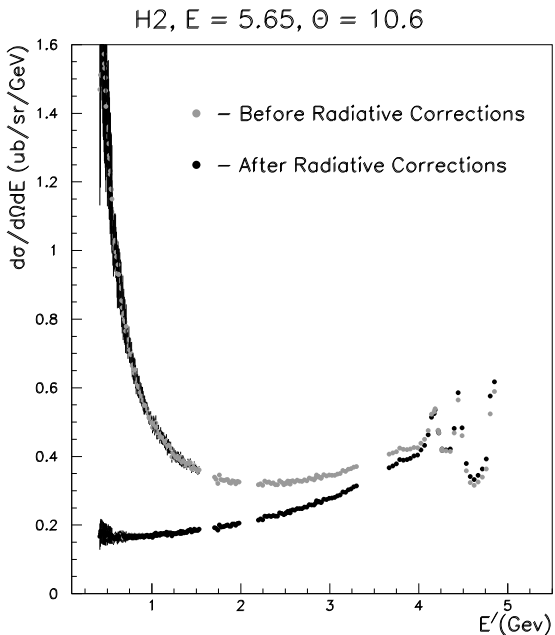


Figure 1. Inclusive scattering of 5.65 GeV electrons on hydrogen,[7] illustrating the magnitude of radiative corrections required.

Electron scattering experiments enjoy a number of benefits. Intense electron beams (over 100 microamps) can be routinely produced and have both an energy spread and uncertainty in absolute energy of  $\Delta E/E < 10^{-3}$ . These beams,

combined with the relatively large cross sections, allow the use of small acceptance spectrometers which have high resolutions, usually  $\Delta p/p < 10^{-3}$ . For experiments of the form,  $A(e, e'X)$  where the scattered electron and a single hadron are detected, two such spectrometers are usually used giving a good missing mass resolution so that exclusive measurements can be performed. In addition to high resolution spectrometers, large acceptance devices such as the CLAS[6] detector, which still has a momentum resolution of about 1%, are used to make measurements covering a large kinematic range or to detect multi-hadron final states.

The ability to do precision experiments with electron scattering does come with a price. Electrons passing through targets produce large fluxes of photons, electrons and positrons at small scattering angles. These fluxes, along with neutrons knocked out of nuclei in beam pipes and beam dumps constitute a large background that is always a challenge to mitigate. For large acceptance or non-magnetic detectors, these backgrounds lead to a limit on the luminosity that a given experiment can tolerate. Much higher luminosities can be reached when well shielded magnetic spectrometers are used, which at the same time limit the kinematic coverage. Thus an experiment that covers a broad range of kinematics (say in  $x$  and  $Q^2$ ) will require many separate physics configurations of the experimental equipment.

As well as creating backgrounds, the ease with which electrons radiate photons leads to large effects that must be corrected. “Internal bremsstrahlung”, in which a scattering electron radiates a real photon while in the Coulomb field of the target particle, as well as effects such as vertex corrections, will modify observed cross sections, generally making them larger than they would be for pure single photon exchange. If an electron radiates before scattering, the exchanged photon will have a smaller  $Q^2$ , giving a larger scattering yield than an un-radiated electron. Thus, with measurements at high energy loss (low  $x$ ), cross sections can be modified by large factors. (See Fig. 1) To make radiative corrections requires a good knowledge of cross sec-

tions being measured and is thus generally an iterative procedure.[8]

### 3. Comparison of Neutrino Monte Carlos to Electron Scattering

The similarities in neutrino and electron scattering suggest that neutrino event generators be modified to generate electron scattering events to compare to electron scattering data. The availability of a variety of electron scattering data with precise measurement of the initial and final states can be used to test the nuclear physics and approximations made in these event generators.

The strong dependence of electron scattering cross sections on  $Q$  ( $\sim 1/Q^4$  relative to neutrino scattering), adds a slight complication to the task of modifying a neutrino Monte-Carlo simulation to produce electron events. One method of dealing with this is to run an event generator with a limit on  $Q^2$  range corresponding to the electron scattering data of interest. The approach taken here is to instead run neutral current scattering with an unmodified event generator and then tag each event with a weight. This weight is the ratio of the electron scattering cross section for the kinematics of the event to the neutrino cross section used for the event.

In the comparisons below, the NUANCE[1] simulation is used to generate Monte Carlo electron scattering “data” to compare to to  $A(e, e')$  and  $^{12}\text{C}(e, e'p)$  from various electron scattering facilities. For the present work, the resonance production and deep inelastic scattering models will be turned off, leaving only neutral current quasi-elastic scattering. However, these techniques could be extended to these reactions or to other neutrino event generators.

#### 3.1. Quasi-elastic electron scattering

The NUANCE event generator implements the relativistic Fermi gas model of Smith and Moniz.[9] This Fermi gas model has also been developed for electron scattering.[10] To test this event generator against single arm inclusive electron scattering, NUANCE is run with a monochromatic neutrino beam and allowed to only generate neutral current quasi-elastic events. The

fermi-momentum and binding energy inputs to the quasi-elastic model are taken from electron scattering data[11] in the usual way.

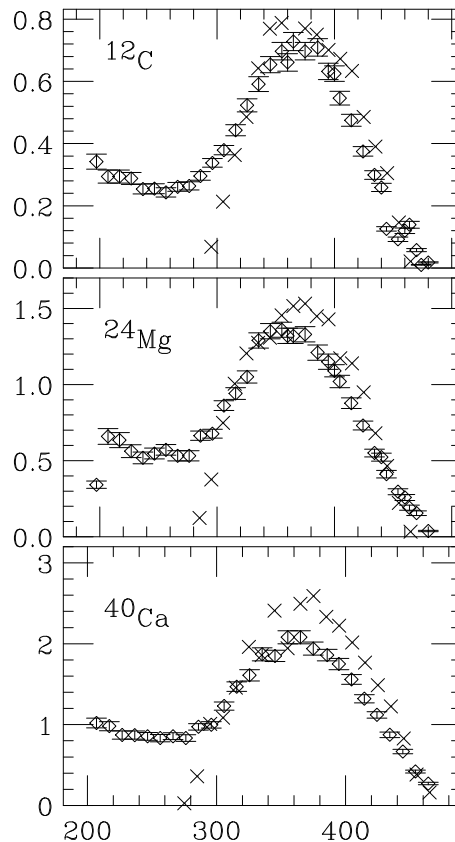


Figure 2. 500 MeV inclusive electron scattering at  $60^\circ$  (diamonds)[12] compared to simulation with NUANCE (crosses). The tails in the data at low scattered electron energies arise from the start of pion production and the breakdown of Fermi gas model.

The resultant event set is compared to a given electron scattering experiment by selecting events where the scattered neutrinos pass through solid angle and momentum apertures equivalent to those used in the experiment. Since single arm electron scattering is usually corrected for radiative effects, these effects are not included in the

simulation. Cross sections are calculated in a standard manner with the exception that each event is weighted by

$$\text{Weight} = \frac{8\pi^2\alpha^2}{G_F^2 Q^4} \frac{W_{\text{electron}}}{W_{\text{neutrino}}} \quad (2)$$

where  $W_{\text{electron}}$  and  $W_{\text{neutrino}}$  are the respective contractions of the lepton and nuclear currents evaluated for the same Fermi gas parameters.

The cross sections obtained with this procedure are compared (Fig. 2) with data for 500 MeV electrons scattered at  $60^\circ$  on several nuclei.[12] The position, width, and magnitude of the simulated quasi-elastic peak agree well with the data, particularly for the lighter nuclei. The good agreement continues at higher electron energies and momentum transfers, although it only applies at the highest scattered electron energies as resonance production increases in relative magnitude and starts to overlap the low momentum side of the quasi-elastic peak.

This agreement is not too surprising, since the Fermi gas parameters were derived from electron scattering and the weight factors out the physics of the neutrino scattering vertex replacing it with the electron vertex. But this comparison does provide a higher resolution check on the implementation of Fermi gas model in NUANCE than is possible by comparing to neutrino scattering. This simple check is also a prerequisite to comparing neutrino event generators to more complicated reactions where hadrons are detected in addition to scattered electron.

### 3.2. Transparency

As neutrino beams are not monochromatic, the neutrino energy for any specific event must be estimated by adding up the energy of the scattered lepton (assuming it has charge) and the hadronic fragments of the struck nucleon or nucleus. As the efficiency of the detection of these fragments can be strongly energy and particle type dependent it is important to include, in neutrino event generators, a simulation of the propagation of these fragments through the nucleus.

The intra-nuclear cascade models used for these final state interaction simulations are tested by comparing them to hadron nucleus scattering

data (where the initial hadron starts outside the nucleus). By looking at electron scattering data, a more analogous comparison to neutrino scattering can be made as the hadrons originate throughout the nuclear volume.

One class of electron scattering measurements that can be used to check these final state interactions models are measurements of ‘‘Transparency’’ made with  $A(e, e'\text{hadron})$  reactions. Transparency is a measure of the probability that a hadron struck or created at the primary scattering vertex, will leave the nucleus essentially undisturbed. Several measurements of  $A(e, e'p)$  have been made [13–17], and  $A(e, e'\pi)$  measurements are planned[18].

The definition of transparency used in recent experiments[14] is

$$T(Q^2) = \frac{\int_V d^3p_m dE_m Y_{\text{exp}}(E_m, \vec{p}_m)}{\int_V d^3p_m dE_m Y_{\text{PWIA}}(E_m, \vec{p}_m)}, \quad (3)$$

where the integral is over the kinematic acceptance of the spectrometers with limits on the missing energy ( $E_m < 80$  MeV) and missing momentum ( $|\vec{p}_m| < 300$  MeV/c).  $E_m = E_e - E_{e'} - T_{p'} - T_{A-1}$  is the unobserved energy, and  $\vec{p}_m = \vec{p}_{p'} - \vec{q}$  is the difference between the detected proton momentum and the momentum transferred by the electron.  $Y_{\text{PWIA}}(E_m, \vec{p}_m)$  is the theoretical yield of  $(e, e'p)$  events with the assumption that the proton does not scatter or get absorbed on its way out of the nucleus. It is proportional to  $\sigma_{ep} S(E_m, \vec{p}_m)$  where  $\sigma_{ep}$  is the off-shell electron-proton cross section and  $S(E_m, \vec{p}_m)$  is the spectra function which is defined as the probability of finding a proton within the nucleus with a separation energy  $E_m$  and momentum  $p_m$ .

A natural way to test proton final state interactions in a neutrino event generator is to treat the simulation events as ‘‘data’’ and using the resulting simulation yield,  $Y_{\text{MC}}$ , instead of the experimental yield  $Y_{\text{exp}}$  in the above equation. To do this properly would require two modifications to the version of NUANCE used here.

Unlike inclusive electron scattering, coincidence  $A(e, e'p)$  usually do not have radiative corrections applied. Instead, these corrections, along with other experimental effects, are usually applied to the theoretical calculations (PWIA here).

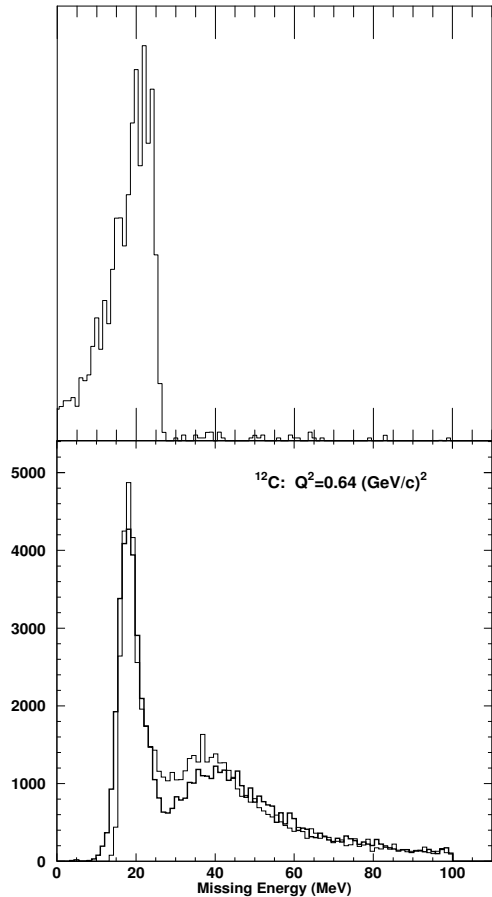


Figure 3. Missing energy spectra of  $^{12}\text{C}(e, e'p)$  at  $Q^2 = 0.64 \text{ (GeV}/c)^2$ . Top: NUAGE simulation, Bottom: Data and PWIA calculation[15,16].

Modifying neutrino event generators to include radiative corrections is quite possible using existing prescriptions[8,19], but beyond the scope of the present work. In addition to the lack of radiative corrections, neutrino event generators usually use a fermi-gas description of the nuclear structure, rather than spectral functions which more accurately reproduce the shell nature of the nucleus.

The lack of radiative corrections is illustrated in Fig. 3 where the data (and PWIA calculation) show a sharp peak at a missing energy of

20 MeV corresponding to knockout of  $p$ -shell protons and a broader peak at 40 MeV corresponding to knockout of  $s$ -shell protons. The broad tail at higher missing energy is due to radiative effects. In contrast, the NUAGE simulation has a single peak at low missing energy and no tail.

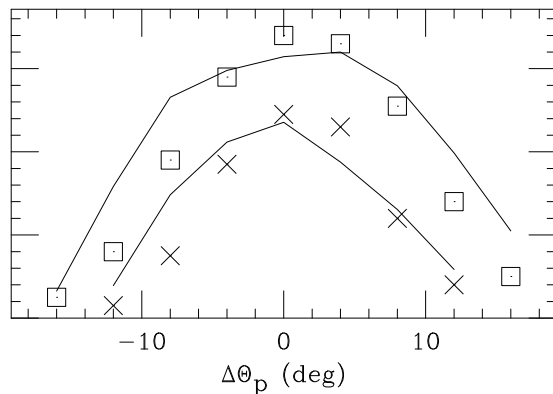


Figure 4.  $^{12}\text{C}(e, e'p)$  Yield vs.  $\theta_p - \theta_q$  for  $Q^2 = 0.64 \text{ (GeV}/c)^2$  (squares) and  $Q^2 = 0.128 \text{ (GeV}/c)^2$  (crosses). Solid lines are predictions from NUAGE, arbitrarily normalized.

Despite the differences in the details of the missing energy spectra, some interesting comparisons can be made by integrating yields over the missing energy ( $E_m < 80 \text{ MeV}$ ). Fig. 4 shows this integrated yield as a function of the angle of the knocked-out proton relative to the direction of momentum transfer. The shapes of angular distributions for the simulation, which arise from the fermi-gas model, agree well with angular distributions of the experimental yields.

An alternate definition of transparency with NUAGE can be used, taking the ratio of simulation yield with final-state interactions turned on to the yield with rescattering turned off. The final-state interaction code in the version of NUAGE used here assumes an  $^{16}\text{O}$  nucleus, so should show a lower transparency (more absorption) than  $^{12}\text{C}$  data. However, the simulation instead underes-

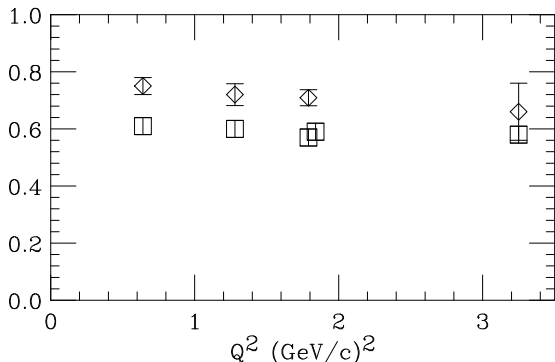


Figure 5. Proton transparency at  $Q^2$  of 0.64, 1.28, 1.79 and 3.25 on  $^{12}\text{C}$ , corresponding approximately to proton kinetic energies of 350, 700, 970 and 1800 MeV. Squares are data[15,16], diamonds are NUANCE simulation described here

estimates the final-state nuclear effects, giving a transparency approximately 20% larger than the data over a broad range of kinematics (proton kinetic energies from 350 to 1800 MeV). (See Fig. 5) If the final-state interaction model can be generalized to any nucleus, it would be interesting to extend the comparison to heavier nuclei. (Transparency data exist for nuclei as heavy as Gold.[17])

#### 4. Conclusion

Neutrino event generators include nuclear physics models that are difficult to validate using neutrino scattering data alone. Because of the similarities in neutrino and electron scattering data, these event generators can be modified to generate electron scattering events which can then be compared to high resolution electron scattering data. A limited comparison, using NUANCE as an example, has been carried out here. This comparison showed, that for the kinematics considered, quasi-elastic scattering on nuclei was reasonably described when only the scattered lepton was considered. However, when also detecting the recoil nucleon from quasi-elastic scattering, this comparison suggests that the final

state interaction model does not contain enough absorption or rescattering of knocked out nucleons.

As more precision neutrino experiments are performed, it would be valuable to extend these to electron scattering in scope and to other neutrino event generators, such as NEUGEN. Adding radiative corrections to event generators will allow more electron scattering data to be compared and allow direct cross sections comparisons, rather than comparisons using ratios as in the above transparency discussion. Extending the neutrino resonance production and deep-inelastic scattering models to electron scattering would also allow comparison to  $A(e, e')$  data such as pion transparency measurements. It is also feasible to make new electron scattering measurements if such measurements could help improve neutrino experiments.

#### 5. Acknowledgments

This work was supported by DOE Contract No. DE-AC05-84ER40150 under which the Southeastern Universities Research Association (SURA) operates the Thomas Jefferson National Accelerator Facility (Jefferson Lab).

#### REFERENCES

1. D. Casper, Nucl. Phys.B (Proc. Suppl) 112 (2002), 161.
2. H. Gallagher (for the MINOS Collaboration), Nucl. Phys.B (Proc. Suppl) 112 (2002), 161.
3. P. A. Souder *et al.*, Phys. Rev. Lett. **65**, 694 (1990).
4. The JLab G0 Experiment, <http://www.npl.uiuc.edu/exp/G0/publicWeb/>.
5. The JLab Qweak Experiment, <http://www.jlab.org/qweak/>.
6. W. Brooks, "Hadronic Multi-particle Final State Measurements with CLAS at Jefferson Lab," these proceedings.
7. Private communication, M. E. Christy. From JLab Hall C experiment E99-118.
8. R. Ent, B. W. Filipone, N. C. R. Makins, R. G. Milner T. G. O'Neill, and D. A. Wasson, Phys. Rev. C **64**, 054610 (2001).

9. R. A. Smith and E. J. Moniz, Nucl. Phys. **B43**, 605 (1972). [Erratum Nucl. Phys. **B101**, 547 (1975)].
10. E. J. Moniz, Phys. Rev. **184**, 1154 (1969).
11. E. J. Moniz, I. Sick, R. R. Whitney, J. R. Ficenec, R. D. Kephart, and W. P. Trower, Phys. Rev. Lett **26**, 445 (1971).
12. R. R. Whitney *et al.*, Phys. Rev. C **9**, 2230 (1974).
13. G. Garino *et al.*, Phys. Rev. C **45**, 780 (1992).
14. N. C. R. Makins *et al.*, Phys. Rev. Lett **72**, 1986 (1994), T. G. O'Neill *et al.*, Phys. Lett. B **351**, 87 (1995).
15. Derek van Westrum, Thesis, University of Colorado (1998).
16. D. Abbott *et al.*, Phys. Rev. Lett. **80**, 5072 (1998).
17. K. Garrow *et al.*, Phys. Rev. C **66**, 044613 (2002).
18. JLab experiment E01-107.
19. J. A. Templon, C. E. Vellidis, R. E. J. Florizone, and A. J. Sarty, Phys. Rev. C **61**, 014607-1 (1999).